

# A Reduced Order Model for Epitaxial Growth

Russel E. Caffisch and David G. Meyer

*This paper is dedicated to Stan Osher on the occasion of his 60th birthday.*

**ABSTRACT.** We formulate a reduced order model for multi-layer, epitaxial growth of a thin film. The model describes layer-by-layer growth using three bulk (i.e. scalar) quantities per layer: average coverage  $\psi$ , average island number density  $n$  and average adatom density  $\rho$  for each layer. The model relies on simplifying assumptions on the geometry of the islands, as well as several approximations for the physical growth processes. We present analytical results on scaling and the relation to rate equations, as well as numerical results comparing this bulk model to a solid-on-solid (SOS) model and an island dynamics model.

## 1. Introduction

Existing models for epitaxial growth are of several types: Atomistic models, such as the Solid-On-Solid model [11], describe growth through the dynamics of an atomistic representation of the crystal using kinetic Monte Carlo. Island dynamics models [1, 2] describe the growth of each atomistic layer, using a continuum description within the layer. Continuum models, including the Villain equation [10], describe growth by a set of PDEs for various field quantities such as adatom density. Bulk models (or rate equations) describe growth through a set of scalar quantities, which are averages over the spatial domain.

The primary examples of a bulk model are cluster dynamics equations [9], since they describe the growth through the number density  $n_s$  for islands of size  $s$ . They have enjoyed great success in describing the features of precoalescent growth of a single layer and in providing qualitative information and understanding, such as scaling properties of the growth.

Extension of cluster dynamics to multi-layer growth has been carried out by Lagally and Karotis [6]. They have used the resulting model to analyze the scaling properties of rough growth. On the other hand, this extension is rather cumbersome, since it involves many variables, i.e. many values of  $k$  for each layer, and many unknown capture numbers.

A related generalized set of rate equations has been formulated by Stoyanov and Markov [7] for the special case of mound growth.

In this paper, we formulate a new bulk model for multi-layer growth which involves only a small number (three) of variables for each layer, and has a small number of coefficients. This model is suitable for application of control methods to growth. A similar model using the same variables but a different set of equations, without a formal derivation, has been presented in [8]. Cohen [3] and Engelmann [4] have formulated even simpler models that captures many features of MBE growth but do not have the scaling properties described below. To distinguish between the different types of models, we refer to this class of models as "bulk models" and use the term "rate equations" to refer to models of cluster dynamics, as in [6, 9], although this nomenclature is not standard.

First, we present a preliminary model, describing the growth of a single layer, in Section 2. Analytic properties of this model are discussed in Section 3. The main subject of this paper is the multi-layer growth model that is formulated in Section 4. Numerical solutions of this model are described in Section 5. These include computational experiments showing the dependence on physical and numerical parameters, as well as numerical investigation of the scaling with respect to  $R = D/F$ . Section 6 contains some conclusions.

This paper is dedicated to Stanley Osher on the happy occasion of his 60th birthday. His research and his friendship have been a great inspiration.

## 2. Bulk Model for Single Layer Growth

Consider epitaxial growth of a single layer including the following processes: deposition and diffusion of adatoms, nucleation of islands through collisions of adatoms, and attachment of adatoms to the islands leading to island growth and coalescence. For simplicity, the attachment of adatoms from on top of the islands is neglected at this point, but it will be included in the multi-layer models formulated below.

We describe this single-layer process through three scalar (i.e. bulk) variables: island coverage  $\psi$ , adatom density  $\rho$  and island number density  $n$ . Precise definitions are that  $\psi$  is the average island area per substrate area,  $\rho$  is the average number of adatoms per uncovered area of the substrate, and  $n$  is the average number of islands per substrate area. The units of  $\psi$ ,  $\rho$  and  $n$  are  $l^0$ ,  $l^{-2}$  and  $l^{-2}$ , respectively.

The model equations are

$$(2.1) \quad \frac{d}{dt}\{\psi + a^2\rho(1 - \psi)\} = a^2F(1 - \psi)$$

$$(2.2) \quad \frac{d}{dt}\psi = (fq + 2m)a^2$$

$$(2.3) \quad \frac{d}{dt}n = m - c$$

in which  $a$  is the lattice constant,  $F$  is the deposition flux,  $q$  is the step edge density,  $f$  is the average flux of adatoms to a step edge,  $m$  is the nucleation rate for new islands and  $c$  is the coalescence rate for islands.

The first of these is just conservation of mass, under the assumption that there is no attachment to the islands from the upper terraces so that the only relevant source of adatoms is due to deposition flux  $F$  on the uncovered terrace of area  $1 - \psi$ . The second equation says that total island area increases due to island

growth and island nucleation. The critical island size is assumed to be 1, so that a single nucleation adds an area of  $2a^2$ . The island growth is just the total flux to the islands, which is the average flux  $f$  multiplied by the total perimeter (i.e. the step edge density)  $q$  of the islands. Finally, the third equation says that the number density of islands increase due to nucleation and decreases due to coalescence.

In order to develop constitutive relations for  $f$ ,  $q$ ,  $m$  and  $c$ , we further define the following:  $b$  is the average island radius,  $r$  is the average distance between islands,  $v$  is the average normal velocity of boundary of a growing island. A simple definition of  $r$  is that it is the average distance to the nearest island from a point outside the islands. We propose the following constitutive equations for these quantities:

$$\begin{aligned}
 (2.4) \quad & v = fa^2 \\
 (2.5) \quad & f = D\rho(r^{-1} + b^{-1}) \\
 (2.6) \quad & m = D\rho^2(1 - \psi). \\
 (2.7) \quad & c = vn/r \\
 (2.8) \quad & b = \sqrt{\psi/n} \\
 (2.9) \quad & q = nb = \sqrt{\psi n} \\
 (2.10) \quad & r = b(1/\sqrt{\psi} - 1)
 \end{aligned}$$

in which  $D$  is the diffusion coefficient for adatoms on a terrace.

The equations for  $b$  and  $q$  come from the simple relations

$$\begin{aligned}
 (2.11) \quad & \psi = nb^2 \\
 (2.12) \quad & q = nb.
 \end{aligned}$$

To derive the formula for  $r$ , note that  $\psi$  is the ratio of an average island area to the average substrate area per island. The average islands area is  $b^2$  and the average substrate area is  $(r+b)^2$ , so that  $\psi = (b/(r+b))^2$  from which this equation follows.

The coalescence rate  $c$  can be calculated as the number density  $n$  of islands multiplied by the rate at which a given island will coalesce with another island. This rate is the inverse time between island collisions, which is the distance between islands  $r$  divided by the island boundary velocity  $v$ . The rate  $c$  in 2.7 can also be interpreted as a three particle interaction between two islands and an adatom, as follows: During coalescence, the island radius  $b$  is larger than the inter-island distance  $r$ , so that the flux  $f$  in 2.5 is approximately  $f = D\rho/r$ . Using 2.9 and 2.10, then 2.7 becomes  $c = a^2 D\rho n^2 (1 - \sqrt{\psi})^{-2}$ . Except for the geometric factor involving  $\psi$ , this is just the rate  $a^2 D$  for hopping times the joint probability  $\rho n^2$  for an adatom and 2 islands to be together.

The nucleation rate per area of the uncovered terrace is just  $D\rho^2$ , since the critical size is assumed to be 1. Since  $m$  is defined as coalescence rate per substrate area, then it has an extra factor of  $1 - \psi$ . The normal velocity  $v$  of an island boundary is just the flux  $f$  of adatoms to the multiplied by the area per atom.

Finally consider the flux  $f$  to the boundary. Since this flux is due to the adatom diffusion, then (ignoring convective effects)

$$(2.13) \quad f = D\mathbf{n} \cdot \nabla\rho$$

This is approximately equal to (ignoring the logarithmic corrections in 2D)  $D\rho/\ell$  in which  $\ell$  is a characteristic length. The natural characteristic length is the island

radius  $b$  for small coverage and the inter-island distance  $r$  for large coverage. So we approximate  $\ell^{-1}$  by  $1/b + 1/r$  to obtain the formula above.

### 3. Properties of the Solution

Here a number of analytic properties of the solutions are described.

#### 3.1. Scaling Properties for the Single Layer Model.

Define the growth parameter  $R = D/F$ , which may be called the inverse Peclet number and is typically very large (i.e.  $10^4 < R$ ). Also define the total coverage variable  $\theta = Ft$ .

The main growth regime is  $R^{-1/2} \ll \theta$ . In this regime, one finds that

$$(3.1) \quad \psi = \psi(\theta) \approx 1 - e^{-\theta}$$

$$(3.2) \quad n = R^{-1/3} \tilde{n}(\theta)$$

$$(3.3) \quad \rho = R^{-2/3} \tilde{\rho}(\theta)$$

Prior to this main growth period, there is an initial transient for  $\theta \ll 1$  in which

$$(3.4) \quad \psi = \psi(\theta) \approx \theta$$

$$(3.5) \quad n = R^{-1/2} \tilde{n}(R^{1/2}\theta)$$

$$(3.6) \quad \rho = R^{-1/2} \tilde{\rho}(R^{1/2}\theta).$$

These scaling properties are same as those of rate equations. In fact as described below, the single layer model is equivalent to rate equations for small coverage.

#### 3.2. Comparison to Rate Equations.

Set  $n_k$  = density of islands containing  $k$  atoms and use  $\theta = Ft$  as time variable. Rate equations are

$$(3.7) \quad \dot{n}_1 = 1 - 2R\sigma_1 n_1^2 - n_1 \sum_{k>1} R\sigma_k n_k$$

$$(3.8) \quad \dot{n}_k = R\sigma_{k-1} n_1 n_{k-1} - R\sigma_k n_1 n_k$$

For capture numbers of  $\sigma_k = \bar{\sigma}$ , these simplify to

$$(3.9) \quad \dot{\rho} = 1 - 2R\bar{\sigma}\rho^2 - R\bar{\sigma}\rho n$$

$$(3.10) \quad \dot{n} = R\bar{\sigma}\rho^2$$

in which  $\rho = n_1$  and  $n = \sum_{k>1} n_k$ .

The reduced order model is approximately equivalent to these rate equations for small coverage  $\theta$ , i.e. in the pre-coalescent regime.

### 4. Bulk Model for Multi-Layer Growth

The single layer model described above can be extended to a multi-layer model by defining the variables separately for each layer. The primary variables are coverage  $\psi_k$ , number density  $n_k$  and adatom density  $\rho_k$ . To be precise these are defined as follows:  $\psi_k$  is the area of the  $k$ th layer per unit substrate area,  $n_k$  is the number of islands on top of the  $k$ th layer (i.e. of height  $k + 1$ ) per unit substrate area, and  $\rho_k$  is the density of adatoms per unit area on the terrace of height  $k - 1$ . This distinction between normalization by substrate area for  $\psi_k$  and  $n_k$  and terrace area

for  $\rho_k$  is natural and usually implicit, but it is important to get the correct scaling below.

The equation

$$(4.1) \quad (d/dt)\psi_k = (q_k(f_k^- + f_k^+) + 2m_k)a^2$$

$$(4.2) \quad (d/dt)n_k = m_k - c_k$$

$$(4.3) \quad (d/dt)(a^{-2}\psi_k + \rho_k(\psi_{k-1} - \psi_k)) = F(\psi_{k-1} - \psi_k) + q_k f_k^+ - q_{k-1} f_{k-1}^+$$

in which, on the terrace of level  $k$ ,  $q_k$  is the step edge density for islands (of height  $k + 1$ ),  $m_k$  is the nucleation rate, and  $c_k$  is the coalescence rate. Each of these is defined per unit substrate area. For the boundary of an island on the  $k$ th terrace (i.e. separating terraces of height  $k$  and the  $k + 1$ ) the flux to the boundary from the lower terrace is  $f_k^-$  and the flux from the upper terrace is  $f_k^+$ .

As in the single layer model, for each layer  $k$  define the average normal velocity  $v_k$  of an island, the average island radius  $b_k$  and the average interisland distance  $r_k$ . The constitutive equations for these quantities are the following, whose derivation is similar to that for the single layer model:

$$(4.4) \quad v_k = (f_k^- + f_k^+)a^2$$

$$(4.5) \quad f_k^+ = D\rho_{k+1}\left(\frac{\bar{r}_+}{r_{k+1}} + \frac{\bar{b}_+}{b_k}\right)(\psi_k - \psi_{k+1})$$

$$(4.6) \quad f_k^- = D\rho_k\left(\frac{\bar{r}_-}{r_k} + \frac{\bar{b}_-}{b_k}\right)(\psi_{k-1} - \psi_k)$$

$$(4.7) \quad m_k = D(\psi_{k-1} - \psi_k)\rho_k^2$$

$$(4.8) \quad c_k = 2\bar{c}v_k n_k / r_k$$

$$(4.9) \quad b_k = \sqrt{\psi_k / n_k}$$

$$(4.10) \quad q_k = \sqrt{n_k \psi_k}$$

$$(4.11) \quad r_k = b_k(\sqrt{\psi_{k-1} / \psi_k} - 1).$$

Here we assume that there is jumping up or down; i.e. attachment to an edge from adatoms on both the upper and lower terraces adjacent to the edge. Set  $a = 1$ . For an edge separating level  $k$  and level  $k + 1$ , denote the flux from lower terrace to the edge as  $f_k^-$  and from upper terrace to the edge as  $f_k^+$ . One can easily show the constants  $F, D, \bar{r}_+, \bar{r}_-, \bar{b}_+, \bar{b}_-, \bar{c}$  are the only parameters that need to be assigned in the model. Any other parameters could be absorbed into the definitions of the variables. The latter five of these parameters are dimensionless.

This is a set of 3 ODEs for each level that is simulated. If the coverage  $\psi_k$  is 0 then there is terrace of height  $k$ , and if  $\psi_k$  is 1 then the  $k$ -th layer is complete. The dynamics of the  $k$ -th layer only occur when  $0 < \psi_k < 1$ , so that a layer with  $\psi_k$  close to 0 or 1 is said to be inactive. We expect that there will be something like 3 active layers at any one time.

## 5. Numerical Results

### 5.1. Multi-Layer Solutions.

We have performed a series of computations for the multi-layer model. Typical results are shown in Figure 1, in which we plot the  $\psi_k$ ,  $n_k$ ,  $q_k$ ,  $\rho_k$  and  $\bar{q}$  defined by

$$(5.1) \quad \bar{q} = \sum_{k=1}^M q_k.$$

The most instructive results are those for the total step edge density, which is approximately equal to the intensity of a RHEED signal. Figure 1 (lower left) shows rapid growth of  $\bar{q}$ , followed by a series of oscillations which mark the initiation and completion of each layer.

This description is confirmed by the plots of  $\psi_k$  and  $n_k$  in Figures 1.

## 5.2. Dependence on Numerical Parameters.

There are three difficulties in numerical solution of these equations. The first is that the system is extremely stiff, since the parameter  $D/F$  is very large. This is easily handled using a standard stiff ODE solver such as ODE23s in Matlab.

The second difficulty is that the system has to be truncated at a finite value of  $M = \max k$ . At the top layer, the dynamics must be changed. We have done this in the following way, which is artificial but no more so than any other method we could propose: Treat the top layer just like the single layer equations; i.e. for  $k = M$  set  $f_M^+ = 0$  so that there is no attachment from adatoms on the layer above layer  $M$ . The results show that the treatment of the top layer affects the layer just below it, but does not extend much further than that.

The third difficulty is that the system has singularities near the initiation and the completion of a layer; i.e., for  $\psi_k \ll 1$  and for  $\psi_{k-1} - \psi_k \ll 1$ . These singularities make the system challenging to use in feedback control design and simulation, and we are still investigating this. However, see [5] for some preliminary results. We have tried various methods for controlling these singularities, and the most effective is to cutoff the dynamics in these two regions. Set two numerical desingularization parameters  $\bar{\psi}$  and  $\lambda$  and truncate the equations in the following way: If  $\psi_{k-1} - \psi_k \ll \bar{\psi}$ , replace the system by

$$(5.2) \quad (d/dt)\psi_k = 0$$

$$(5.3) \quad (d/dt)n_k = -\lambda n_k$$

$$(5.4) \quad (d/dt)\rho_k = 0$$

In addition, for this  $k$ , set

$$(5.5) \quad f_{k-1}^+ = 0$$

i.e. do not allow any flux from layer  $k$  to layer  $k-1$ . The reason for including the artificial decay term  $\lambda n_k$  in the equation for  $n_k$  is to ensure that  $n_k$  and  $q_k$  go to 0 as the layer completes. In addition if  $\psi_k \ll \bar{\psi}$ , set

$$(5.6) \quad f_k^+ = 0$$

Computational experiments show that the results, such as the total step edge density  $\bar{q}$  (defined in 5.1) are approximately independent of the parameters  $\bar{\psi}$  and  $\lambda$  over a reasonable range  $.00001 < \bar{\psi} < .01$  and  $1 < \lambda < 20$ . This is illustrated in the following three figures.

We have also examined the dependence on other parameters in the model. Figure 2 shows that the results are independent of the number  $N$  of layers used in the model, at least for the values of  $k$  with  $k < N/2$ .

Figure 3 shows that the results are independent of the cutoff parameter  $\bar{\psi}$  for a range sufficiently small values

Figure 4 shows that the results are independent of the parameter  $\lambda$  which is used to artificially cutoff the  $n_k$ .

The density  $\rho_k$  is the quantity that is most sensitive to the numerical parameters discussed above. On the other hand, the density could be omitted from most of the computation, since adatoms nearly go directly from deposition to attachment. In fact, a related model including only  $\psi_k$  and  $n_k$  provides almost the same results as the model discussed here. It only fails when a layer is initiating. Also, we have included  $\rho$  for comparison to rate equations.

### 5.3. Dependence on Physical Parameters.

Figure 5 shows the dependence on the parameter  $\bar{c}$  which multiplies the coalescence rate  $c$ . This shows that the shape of the oscillations becomes more pointed as  $\bar{c}$  increases.

Figure 6 shows the dependence on the parameters  $\bar{b}_m$  which multiplies the  $1/b$  term in the flux rate  $f_m$ . This shows that the amplitude of the oscillations is smaller for larger values of  $\bar{b}_m$ .

Figure 7 shows the dependence on the parameters  $\bar{b}_p$  which multiplies the  $1/b$  term in the flux rate  $f_p$ . This shows that the amplitude of the oscillations is larger for larger values of  $\bar{b}_p$ .

Figure 8 shows the dependence on the parameters  $\bar{r}_m$  which multiplies the  $1/r$  term in the flux rate  $f_m$ . This shows that the amplitude of the oscillations is smaller for larger values of  $\bar{r}_m$ .

Figure 9 shows the dependence on the parameters  $\bar{r}_p$  which multiplies the  $1/r$  term in the flux rate  $f_p$ . This shows that the amplitude of the oscillations is larger for larger values of  $\bar{r}_p$ .

### 5.4. Scaling Properties for the Multiple Layer Model.

We have performed a series of computations of the multi-layer model for values of  $R$  ranging from  $10^3$  to  $10^8$ . Figure 10 (upper) presents the total step edge density  $\bar{q}$  as a function of time  $t$  for different values of  $R$  on a semi-logarithmic plot. Note that the shape of the curves is nearly independent of  $R$  except for a shift. For each time  $t$ , we approximate  $\bar{q}$  by a power law function  $cR^{-\alpha}$ , using a least square linear fit to  $\log(\bar{q})$ , in which  $c = c(t)$  and  $\alpha = \alpha(t)$ . The resulting power  $\alpha$  as a function of time  $t$  is plotted in Figure 10. Its value is approximately 1/6 for most  $t$ , but near the completion of each layer it is approximately 1/5. The value 1/6 is in agreement with rate equations. The validity of the fit is demonstrated in Figure 10, in which we plot  $\bar{q}/cR^{-\alpha}$ , for each value of  $R$ .

## 6. Conclusions

The single layer and multi layer models formulated above have been shown to provide qualitative agreement with results from simulation of epitaxial growth. This model is much simpler than a full PDE model, such as island dynamics, but it naturally extends to multiple layers. On the other hand, so far we have not succeeded in obtaining the coarsening and roughening that accompanies multi-layer growth.

## References

- [1] W.K. Burton, N. Cabrera, and F.C. Frank. The growth of crystals and the equilibrium structure of their surfaces. *Phil. Trans. Roy. Soc. London Ser. A*, 243:299–358, 1951.
- [2] R.E. Caffisch, M. Gyure, B. Merriman, S. Osher, C. Ratsch, D. Vvedensky, and J. Zinck. Island dynamics and the level set method for epitaxial growth. *Applied Math. Lett.*, 12:13–22, 1999.
- [3] P.I. Cohen, G.S. Petrich, P.R. Pukite, G.J. Whaley, and A.S. Arrott. Diffraction oscillations from low index surfaces. *Surface Sci.*, 216:222–248, 1989.
- [4] A. Engelmann. *Modeling and Trajectory Morphing of Epitaxial Thin-Film Growth Systems*. PhD thesis, Department of Electrical and Computer Engineering, University of Colorado, 2000.
- [5] A. Engelmann, D.G. Meyer, J.E. Hauser, and R.E. Caffisch. Trajectory morphing applied to epitaxial thinfilm growth. In *Proceedings of the 1999 American Control Conference*, pages 3589–3593, 1999.
- [6] R. Kariotis and M.G. Lagally. Rate equation modelling of epitaxial growth. *Surface Science*, 216:557–578, 1989.
- [7] S. Stoyanov and I. Markov. On the 2d-3d transition in epitaxial thin film growth. *Surface Sci.*, 116:313–337, 1982.
- [8] J. Y Tsao. *Material Fundamentals of Molecular Beam Epitaxy*. Academic Press, Boston, 1994.
- [9] J. Venables. Rate equation approaches to thin film nucleation kinetics. *Phil. Mag.*, 27:697–738, 1973.
- [10] J. Villain. Continuum models of crystal growth from atomic beams with and without desorption. *J. de Phys. I*, 1:19–42, 1991.
- [11] J.D. Weeks and G.H. Gilmer. Dynamics of crystal growth. *Adv. Chem. Phys.*, 40:157–228, 1979.

MATHEMATICS DEPARTMENT, UCLA.  
*E-mail address:* `caflisch@math.ucla.edu`.

ECE DEPARTMENT, U. OF COLORADO.  
*E-mail address:* `David.Meyer@Colorado.EDU`



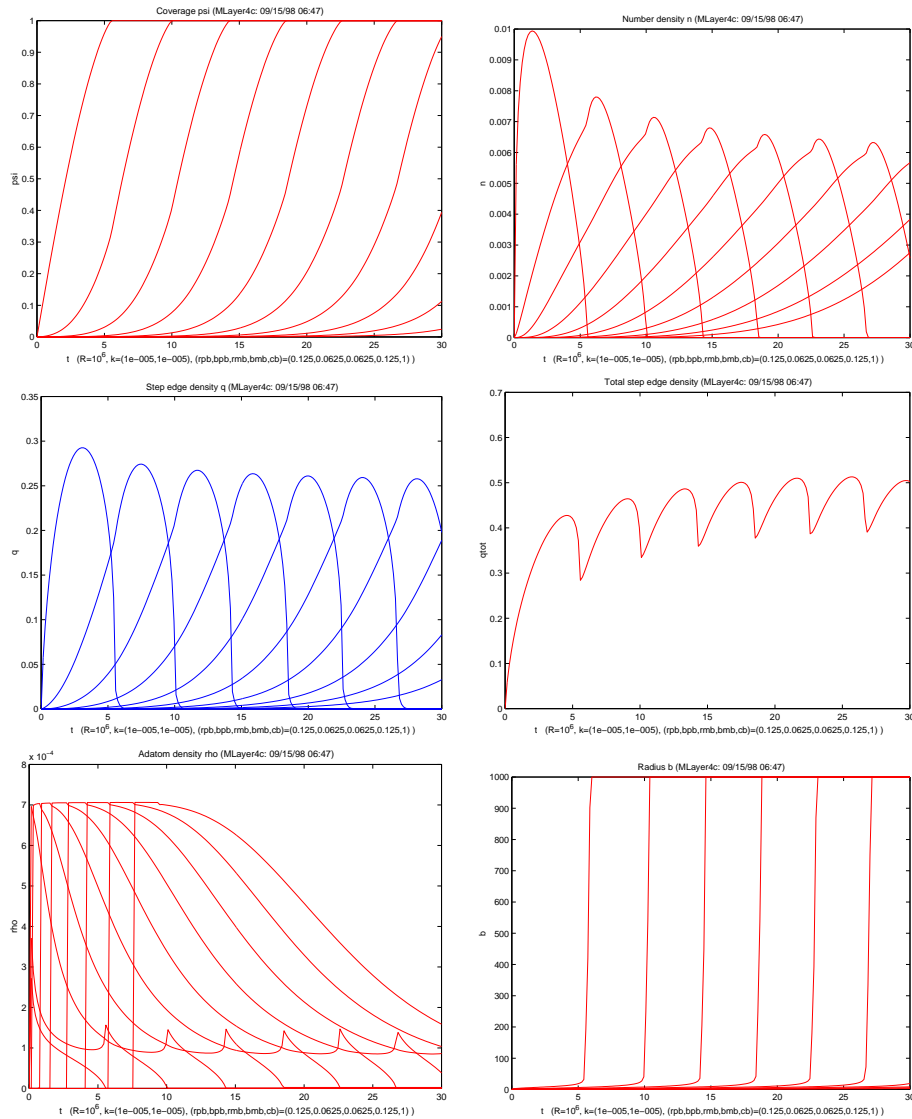


FIGURE 1. Results from multi-layer model with physical parameters  $F = .25$ ,  $D = 10^6 F$ ,  $\bar{r}_+ = \bar{b}_- = 1/8$ ,  $\bar{r}_- = \bar{b}_+ = 1/16$ ,  $\bar{c} = 1$  and with desingularization parameters  $\lambda = 10$  and  $\bar{\psi} = .001$ . Plotted are island coverage  $\psi_k$  (upper left), island number density  $n_k$  (upper right), step edge density  $q_k$  (middle left), total step edge density  $\bar{q}$  (middle right), adatom density  $\rho_k$  (lower left) and island radius  $b_k$  (lower right).

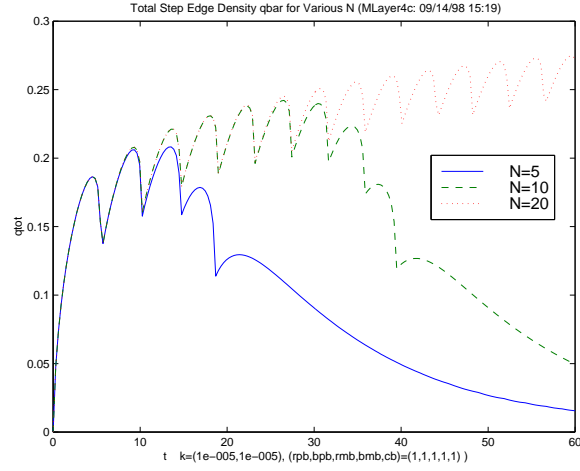


FIGURE 2. Total step edge density vs.  $t$  from multi-layer model, for various values of  $N$ . This shows that the results for  $k < N/2$  are independent of  $N$ .

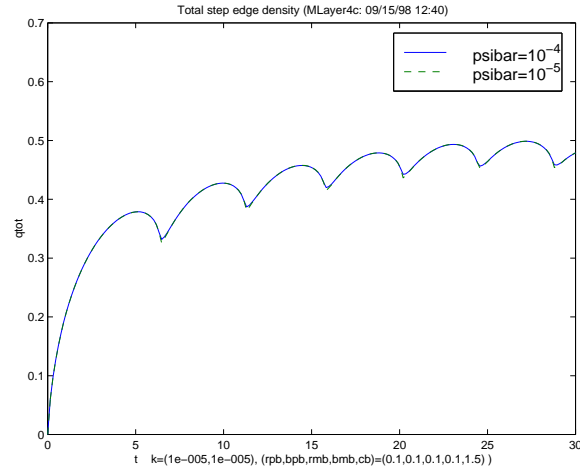


FIGURE 3. Total step edge density vs.  $t$  from multi-layer model, for various values of  $\bar{\psi}$ . This shows that the results are independent of  $\bar{\psi}$ .

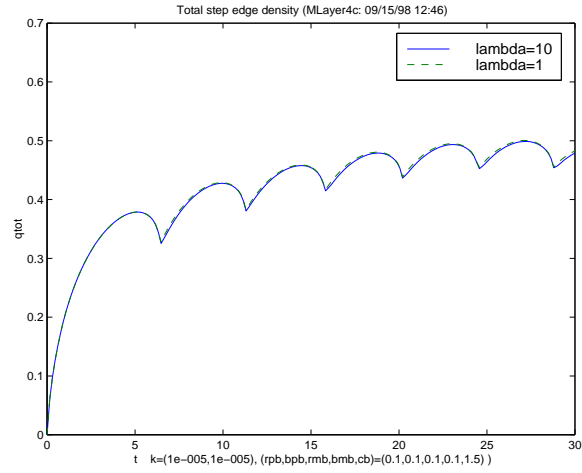


FIGURE 4. Total step edge density vs.  $t$  from multi-layer model, for various values of  $\lambda$ . This shows that the results are independent of  $\lambda$ .

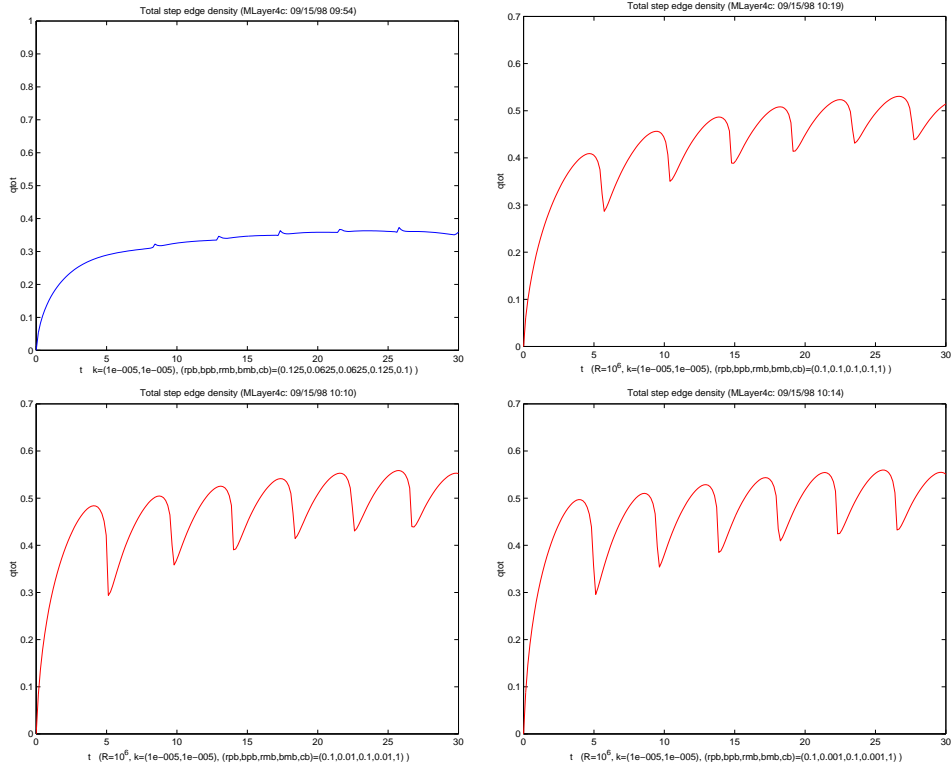


FIGURE 5. Total step edge density vs.  $t$  from multi-layer model, for various values of  $\bar{c}$ .  $\bar{c} = 10$ . (upper left),  $\bar{c} = 2$ . (upper right),  $\bar{c} = .5$  (lower left) and  $\bar{c} = .1$  (lower right). The other parameters are held fixed at  $\bar{r}_+ = \bar{b}_- = 1/8$ ,  $\bar{r}_- = \bar{b}_+ = 1/16$ .

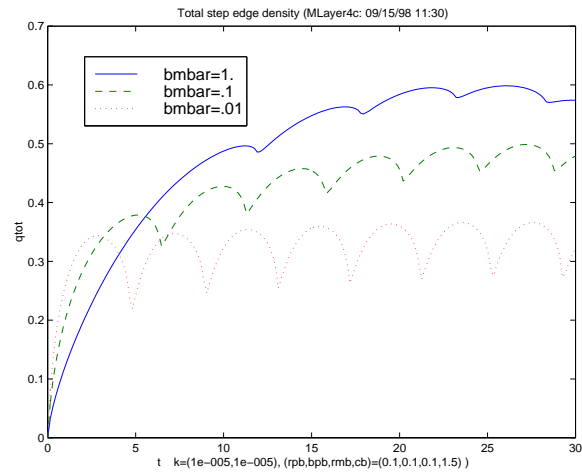


FIGURE 6. Total step edge density vs.  $t$  from multi-layer model, for various values of  $\bar{b}_m$ . The other parameters are held fixed at  $\bar{r}_+ = \bar{r}_- = \bar{b}_+ = .1$  and  $\bar{c} = 1$ .

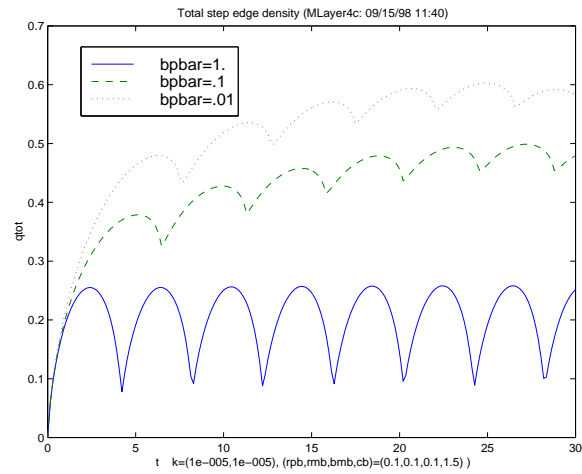


FIGURE 7. Total step edge density vs.  $t$  from multi-layer model, for various values of  $\bar{b}_p$ . The other parameters are held fixed at  $\bar{r}_+ = \bar{r}_- = \bar{b}_- = .1$  and  $\bar{c} = 1$ .

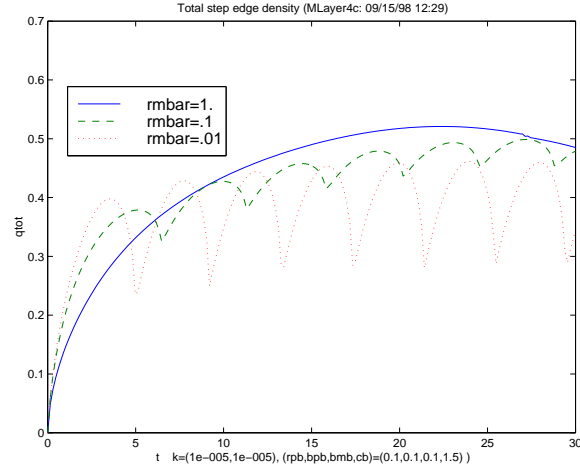


FIGURE 8. Total step edge density vs.  $t$  from multi-layer model, for various values of  $\bar{r}_m$ . The other parameters are held fixed at  $\bar{b}_- = \bar{r}_- = \bar{b}_+ = .1$  and  $\bar{c} = 1$ .

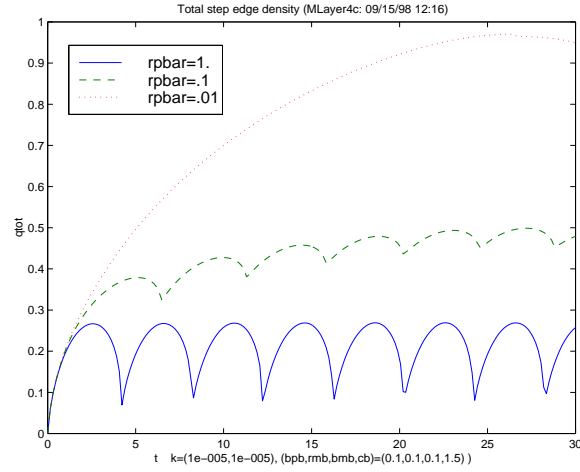


FIGURE 9. Total step edge density vs.  $t$  from multi-layer model, for various values of  $\bar{r}_p$ . The other parameters are held fixed at  $\bar{r}_+ = \bar{b}_- = \bar{b}_+ = .1$  and  $\bar{c} = 1$ .

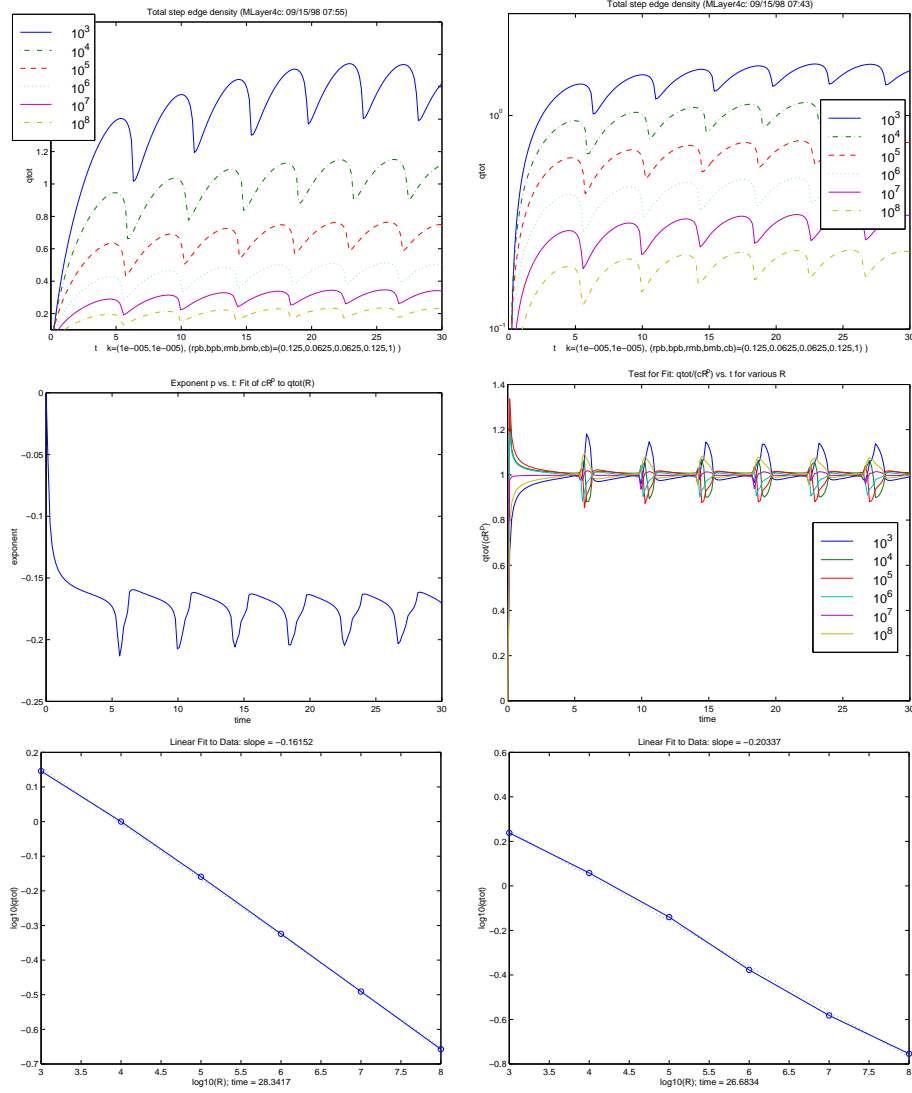


FIGURE 10. Total step edge density  $\bar{q}$  vs.  $t$  from multi-layer model, for various values of  $R = D/F$ . Linear (upper left) and semilog (upper right) plots of  $q$  vs.  $t$ ; exponent  $\alpha$  vs.  $t$  in power law fit  $\bar{q} \approx cR^\alpha$  (middle left);  $\bar{q}/(cR^\alpha)$  vs.  $t$  as a test of power law fit (middle right); linear fit to  $\log \bar{q}$  for  $t = 28.34$  which is the time of the best fit (lower left) and for  $t = 26.68$  which is the time of the worst fit (lower right). The other parameters are held fixed at  $F = 0.25$ ,  $\bar{r}_+ = \bar{b}_- = 1/8$ ,  $\bar{r}_- = \bar{b}_+ = 1/16$  and  $\bar{c} = 1$ .